

FULL PAPER

Embedded Ag NPs in Cysteine-Poly (acrylic acid) Hydrogel with Antibacterial Activity

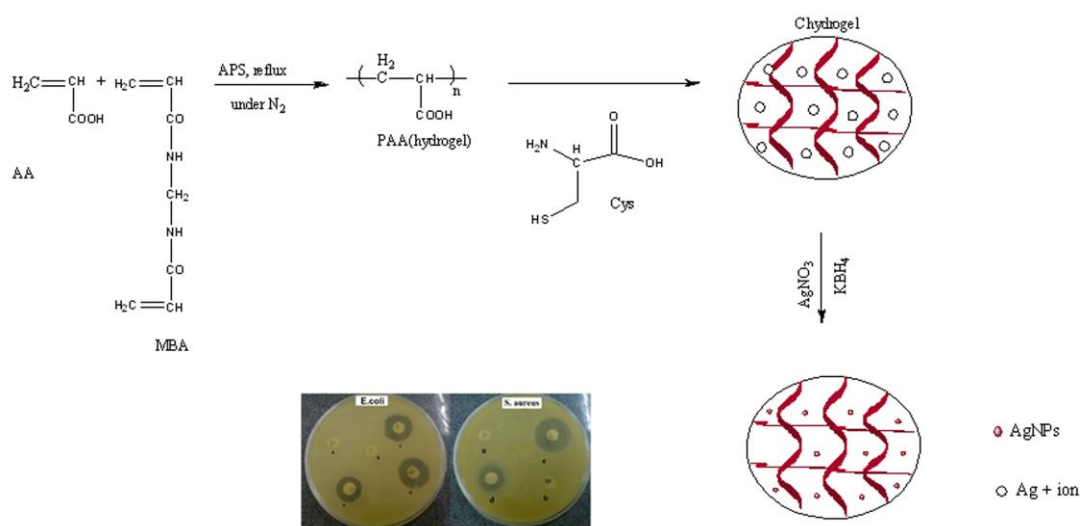
Soghra Fathalipour^{a,*}, Mahdiye Ghanbarizadeh^a

^aDepartment of Chemistry, Payame Noor University, PO Box: 19395-3697, Tehran, Iran Received: 09 May 2018, Revised: 07 June 2018 and Accepted: 22 June 2018.

ABSTRACT: In this research, Ag NPs were loaded on cysteine modified poly(acrylic acid) (PAA) hydrogel. Obtained cysteine-hydrogel (Chydrogel) having different functional groups could stabilize Ag NPs better than un-modified hydrogel due to the presence of disulfid bondings. First, obtained PAA hydrogel from radical polymerization was conjugated with cysteine-hydrochloride (Cys) through amidation reaction and then was used as a substrate and stabilization reagent for Ag ions. Ag ions were reduced on Chydrogel in the presence of NaBH₄ as reducing reagent. The resultant nanocomposite was well characterized by using UV-vis, FT-IR, XRD and SEM techniques. Furthermore, the resultant Ag NPs on the surface of Chydrogel showed high antibacterial behavior against Gram-negative E. coli and Gram-positive S. aureus due to the high reaction of thiol-functions with the outer cell surface.

KEYWORDS: hydrogels, composites, antibacterial, inorganic materials, Ag NPs.

GRAPHICAL ABSTRACT:



1. Introduction

Metal nanoparticles (NPs) have attracted considerable attention in nanotechnology because of their applications in various

fields for example photonic, electronic, catalytic, chemical and biosensor[1-4]. Among metal NPs, AgNPs are very important due to their unique

*Corresponding author: Soghra Fathalipour, Email: s.fathalipour@pnu.ac.ir

physical, chemical properties and antibacterial performance [5-9]. Ag NPs have showed higher antibacterial property than their bulk form against bacteria, virus, and fungi [10,7]. But, in aqueous phase, there are some drawbacks accompanying with their use for antibacterial applications. For example, because of the rapid oxidation and aggregation of Ag NPs, it is hard to control the size; shape and stability of nanoparticles. Different procedures have been used to prepare monodispersed Ag NPs; most cases include the stabilization of the nano particles by surfactants or polymers [11,8,7]. AgNP composites have been synthesized by loaded metal ions into thin films of titania, graphene nanocomposites, porous and natural polymers, which are appropriate for biomedical purposes [12-16,9]. Studies on silver nanoparticles showed that hydrogel polymers are suitable choices for the preparation of nanoparticles in aqueous phase due to the treatment of wound burnings in the form as such [17,18]. Hydrogels are crosslinked hydrophilic networks which are capable to retain a large amount of water due to the presence of several functional groups in the polymers [19,18]. Ag NPs can be loaded

into the hydrogel via the mixing of nanoparticles with the synthesized hydrogel, by the addition of nanoparticles during the gelation process or loading in the swelling process of the hydrogel [13,20]. The functional groups of hydrogel can interact with silver ions and act as anchoring agent to obtain a uniform distribution of nanoparticles [21,22]. Controlled size and uniformed distribution of nanoparticles depend on the number of functional groups within the hydrogel matrix [23]. Silver-hydrogel composites were synthesized by various methods. Varaprasad *et al.* prepared Ag-hydrogel nanocomposite through reduction of silver nitrate in the course of polymer gelation [24]. Fullenkamp *et al.* prepared antibacterial hydrogels through the reaction of Ag(I) and a modified PEG polymer [25]. Also, Sahraei and coworkers synthesized Ag NPs with antibacterial activity on modified gum tragacanth/graphene oxide composite hydrogel [26].

Thiolated hydrogels such as cysteine-poly(acrylic acid) hydrogel might also be a useful method for synthesizing of uniformed antibacterial Ag NPs due to the (a) surface stabilization of nanoparticles through disulfide bonding; (b) thiol-functions

which react with the outer cell surface leading to an improved absorptive endocytosis; and (c) comparatively low toxicity. In this work, Ag NPs were prepared in cysteine modified poly (acrylic acid) (PAA) hydrogel networks. PAA hydrogel was prepared via radical polymerization in the presence of a cross linking agent and, then, was modified by cysteine via the formation of amide bonds between cysteine and hydrogel networks. The resulted hydrogel network was used as template for nucleation and growth of Ag NPs. The resulted nanocomposite was evaluated using UV-vis, FT-IR spectroscopy, X-ray diffraction (XRD) and scanning electron microscopy (SEM). Moreover, It was also examined the antibacterial properties of the prepared nanocomposite. The details of the investigation were presented below.

2. Experimental

2. 1. Materials

Acrylic acid (AA), ammonium persulfate (APS), 1-ethyl-3-(3-dimethylaminopropyl) carbodiimide hydrochloride (EDAC), N,N'-methylenebisacrylamide (MBA), sodium borohydride (NaBH_4), silver nitrate (AgNO_3) were purchased from Merck, Germany. L-cysteine hydrochloride hydrate (Cys) was supplied from Sigma-Aldrich,

Steinheim, Germany. Acrylic acid was distilled under reduced pressure and other reagents were used as received without further treatment. All solutions were prepared with double distilled water.

2.2. Methods

2.2.1. Preparation of Cysteine-Poly (acrylic acid) Hydrogel (Chydrogel)

First, poly (acrylic acid) hydrogels were prepared by following simultaneous redox cross-linked polymerization technique similar to a method described [27]. Resultant hydrogel was modified with cysteine similar to the method previously described for cys-PAA [28]. 1g of the resultant hydrogel was hydrated in 80 ml deionized water and, then, carboxylic acid moieties of polymer were activated by the addition of 0.5 g of EDAC in a final concentration of 50mM. After 15 min of incubation at room temperature, 1 g of Cys was added and the pH-value of the reaction mixture was adjusted to 5 with 2 M NaOH. The reaction mixture was further stirred at room temperature for 3 h under nitrogen atmosphere. The resulting modified hydrogel (Chydrogel) was, then, purified by dialyzing against 1mM HCl two times, additionally two times against 0.5mM HCl containing 1% NaCl and again two times

against 1mM HCl. After dialysis, the pH of Thydrogel was adjusted to 5 with 1 M NaOH and the polymer solution was dried by lyophilisation at -50 °C and 0.01 mbar. Resulted Chydrogel was stored at 4°C until further use. As compared to vacuum-dried hydrogels, lyophilized hydrogels display higher swelling ratios, so resulted hydrogels were lyophilized at -50 °C and stored at 4 °C [6].

2.2.2. Synthesis of silver NPs on the Chydrogel and hydrogel

The obtained Chydrogel and hydrogel (0.1 g) were swelled in distilled water (50 ml) at room temperature for 2 days and, then, the swollen hydrogels were poured into 50 mL of aqueous 5mM AgNO₃ solution and kept for 24 hours to absorb the silver salt. Then, the silver salt-loaded hydrogels were mixed with 50 ml of cold aqueous NaBH₄ solution (1mM) and kept for 2 hours at 4°C. After mixing, a color change to (dark brown/black) color was observed, which approved the formation of silver nanoparticles. The synthesized nanocomposite (10 mg) was dispersed in distilled water (100 ml) through ultrasonic waves for about 30 min and used for antibacterial test.

2.3. Characterization and analysis

The swelling behavior of the resulted hydrogels, before and after loading of silver NP inside the networks, was defined via calculating the ratio (Q) of the hydrogels following Eq (1):

$$Q = W_e / W_d \quad (1)$$

W_e is the weight of the swollen hydrogel and W_d is the dryweight of the pure hydrogel. UV-Vis absorption spectra of the hydrogel-silver nanocomposites were studied on a PG Instruments T80 UV-Vis spectrophotometer with a scan range of 200–800 nm. To carry out this analysis, samples (10 mg/ml) were put in distilled water for 2 days, then Ag NPs were extracted by centrifuging at 1000 rpm for 30 min, and the supernatant was used. X-ray diffraction measurements were recorded using a SIEMENS (D5000) X-ray diffractometer (Cu radiation, $\lambda = 0.1546$ nm) at a 10°/min scanning speed from 2° to 70° (in 2 θ). FT-IR analysis was studied on a Shimadzu 8400 Fourier transform spectrometer in the range of 400–4000 cm⁻¹ using KBr pressed disks. Surface morphologies of resulted hydrogels were studied using HITACHI, 4160 scanning electron microscope (SEM). Antibacterial activity of Ag-hydrogel nanocomposites have been investigated against *Escherichia coli* (*E. coli*) and

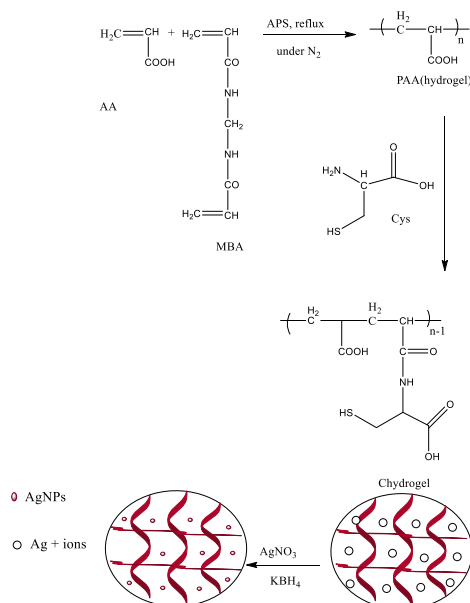
Staphylococcus aureus (*S. aureus*) as models of Gram-positive and Gram-negative bacteria, respectively. The antibacterial activity of Ag nanocomposites was investigated by two methods. The first method is minimum inhibitory concentration (MIC) method and the second is Disk diffusion method. MIC of r nanocomposites was defined via Broth-dilution method. In the disk diffusion method, on the base of MIC of Chydrogel-Ag nanocomposite, samples were made into a disk, and were placed on *E.Coli* and *S. aureus* cultured agar plates. Agar plates were incubated at 37°C for 24h and the diameters of inhibition growth zones were determined.

3. Results and discussion

Scheme 1 illustrates the preparation mechanism of Chydrogel and silver nanoparticles within the swollen hydrogel networks.

Fig. 1A shows the swelling characteristics of the resulted samples. After the

modification of hydrogel and interaction with Ag NPs, significant variation in the swelling capacity of Chydrogel and its composite was appeared. As can be seen, with modification of hydrogel swelling ratio on hydrogel increased and this could be related to the increasing of polar groups (–SH, –S–S, –OH, –CONH₂, –COO[–] and Na⁺) in polymeric chains. The presence of the ionic groups in polymer chains of Chydrogel increased also considerably the swelling ratio. With the inserting of silver nanoparticles inside the PAA hydrogel, the swelling capacity of the gels increased due to the presence of more free spaces. This performance was showed for many of the hydrogel–silver nanocomposites [29,17]. While, the swelling capacity of Thydrogel-Ag is considerable lower than Chydrogel and this could be related to the high interaction of Ag NPs with polar groups [30-33].



Scheme.1. Synthetic scheme for the preparation of the Thydrogel-Ag NPs composite.

The UV-vis of the hydrogel–silver and Chydrogel-Ag nanocomposite are shown in Fig. 1B. The hydrogel–silver and Chydrogel–silver nanocomposites showed an absorption peak at 420 nm, which is related to the surface Plasmon resonance (SPR) of silver NPs. The SPR bands of metal nanoparticles are sensitive to a number of factors, such as particle size, size distribution, shape, and the nature of the surrounding media [27]. Comparing with Ag NPs in the hydrogel, a weak peak is seen

for Ag NPs in the Chydrogel matrix which this could be related to low concentration of extracted Ag NPs because of high interaction between thiol groups of Thydrogel and Ag NPs. These results confirmed the formation of silver nanoparticles in the hydrogel networks and also showed that Chydrogel is a good stabilizing agent for silver NPs in comparison to hydrogel.

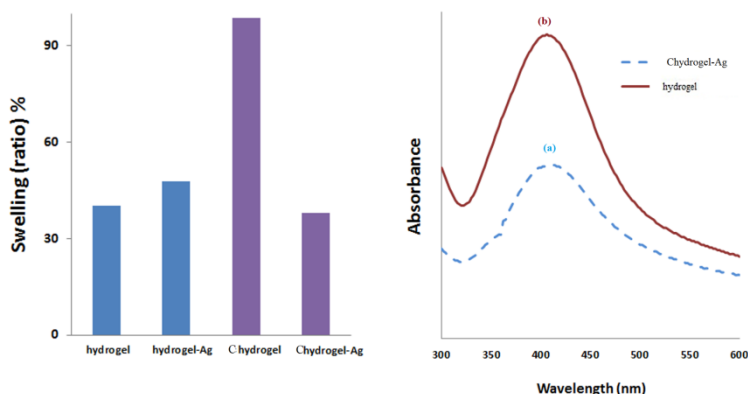


Fig. 1. A: Swelling behavior of pure hydrogel, Chydrogel, Ag-hydrogel and Ag-Chydrogel nanocomposites and B: UV-Vis spectra analysis of hydrogel–Ag and Chydrogel–Ag nanocomposites.

The XRD patterns of the Chydrogel and Chydrogel-Ag nanocomposite are displayed in Fig. 2. In XRD pattern of pristine Chydrogel is appeared a diffraction peak at $2\theta = 13^\circ$ which is attributed to the polymer chains [34] (Fig.2). The XRD data indicated well-defined characteristic patterns of the silver NPs. In XRD pattern of nanocomposite, four diffraction peaks at 2θ values of about 38.1, 44.26 and 64.50 are related to (111), (200) and (220) Bragg's reflection of silver structure[35,36]. The average particle sizes (D) were determined from the Ag (111) diffraction line using Scherrer's equation, $D = k\lambda/\beta\cos\theta$, where k is particle shape factor (generally taken as 0.89), λ is the wave length of $\text{CuK}\alpha$

radiation ($\lambda = 1.54 \text{ \AA}$), θ is the diffraction angle, and β is the full width at half maximum (FWHM) of the diffraction peak[37]. The calculated average size of silver is about 7 nm (FWHM = 1.072°). Meanwhile, in the XRD pattern of nanocomposite, a diffraction peak of polymer is appeared with high intensity at $2\theta: 11^\circ$ that is related to high crystallinity of polymer chains in composite in the presence of Ag NPs.

Fig. 3 represents FT-IR spectra of the hydrogel, Chydrogel, hydrogel-Ag and Chydrogel-Ag nanocomposites. In the FT-IR spectrum of hydrogel, the bands at 3450, 2959, 1740, 1633, 1364, and 1180 cm^{-1} are attributed to the stretching vibration of OH,

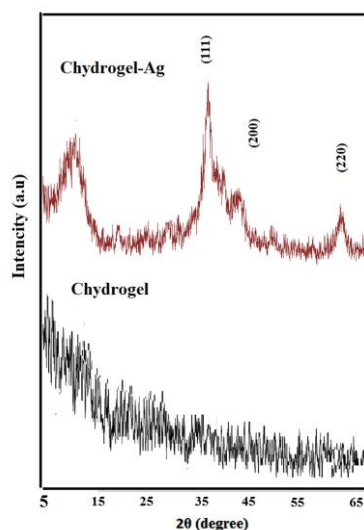


Fig. 2. XRD pattern of Chydrogel and Chydrogel–Ag nanocomposites.

CH (aliphatic), C=O (carboxylic acid), C=O and bending vibration of OH group, respectively[38]. The bands of hydrogel (amide group of crosslinking), C–O–C

were observed in the FT-IR spectra of Chydrogel with differences. In the FT-IR spectra of Chydrogel, the stretching and bending vibration of OH group had red shift comparing with similar bands of hydrogel, which this could be related to thiolated groups. Also, in the FT-IR spectrum of Thydrogel, characteristic peaks around 1449 and 1408 cm^{-1} are related to asymmetric and symmetric stretching modes of carboxylate groups. C=O stretching of carboxylic acid and amid overlapped and appeared at 1667

cm^{-1} and this could be related to the presence of Cys groups. On the other hand, the modification of hydrogel with Cys can be confirmed by the appearance of absorption bands of S-H and C-S stretching vibration at 2540 and 626 cm^{-1} , respectively. After the loading of Ag NPs into hydrogel and Chydrogel, all of the bands had a little red shift comparing with bands of hydrogel and Thydrogel which these results could be related to the some doping effect of metal nanoparticles in the polymer matrix [39].

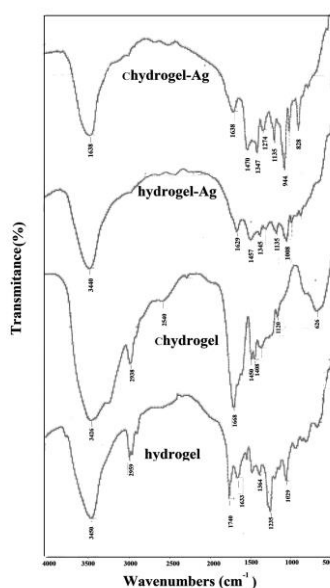


Fig. 3. FT-IR spectra of hydrogel, Chydrogel, hydrogel–Ag and Chydrogel–Ag nanocomposites.

Fig. 4 demonstrates the SEM images of hydrogels and hydrogels containing silver NPs. The image of pristine hydrogel is like arumen (Figs 4a, b) which with modification of hydrogel, its structure

changes. SEM of Chydrogel is in the form of networks with particles on surface them (Figs 4c, d). Obtained changes are attributed to the interactions between new functional groups and this clearly confirms the

modification of hydrogel. The size of pores of networks is between 250 and 650 nm and these nanopores could allow water molecules diffuse in chydrogel (Fig. 4c,d). For comparison, SEM images of Chydrogel networks before adjusting pH are shown in insets of Figs 4c, d. The images represent thick interlock network with various holes. Based on the SEM images, pH of Chydrogel was adjusted and then was used as substrate in synthesis of Ag NPs. With loading of Ag NPs into hydrogels, the morphologies of hydrogels change. SEM images (Figs 4e, f) clearly indicate the formation of Ag NPs on polymer chains rather than just entrapment in the gel networks. On the other hand, by modifying the hydrogel network architecture, difference structure of Ag NPs was obtained.

The resulted Ag NPs on the hydrogel and Chydrogel are as attached spherical and rod like nanoparticles, respectively (Fig 4e-f).

The study of antibacterial activity of samples through MIC method display that hydrogel and Chydrogel have no activity against bacteria, while synthesized Ag NPs on hydrogel networks show high antibacterial activity. MIC of resultant Chydrogel-Ag were 5 and 2.5 $\mu\text{g/ml}$ and for hydrogel-Ag were 20 and 5 $\mu\text{g/ml}$ against *E.coli* and *S. aureus*, respectively. The comparison of all samples displays that the antibacterial activity is attributed to the presence of Ag NPs. These results showed the antibacterial behavior of resultant Ag NPs on Chydrogel is higher than those of hydrogel-Ag nanocomposites.

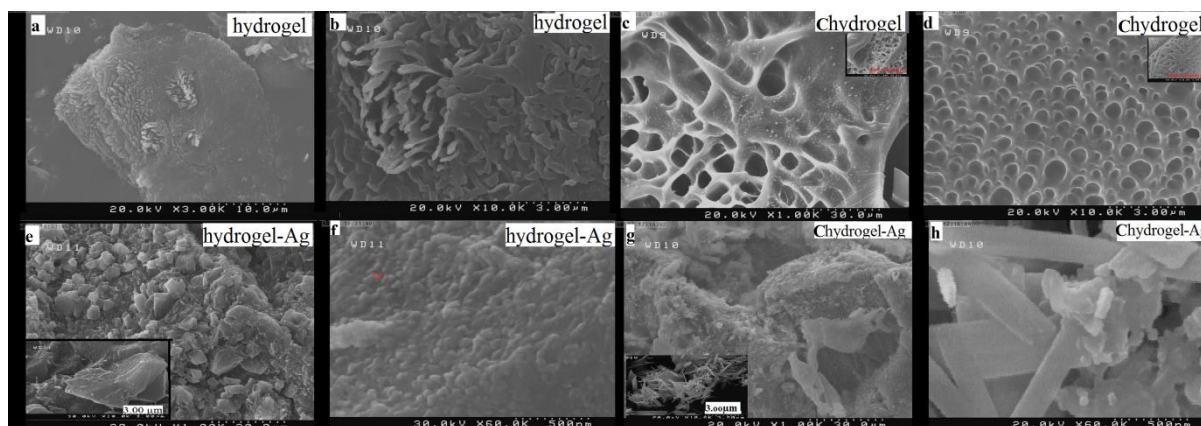


Fig. 4. SEM images of hydrogel (a and b), Chydrogel (c and d), hydrogel-Ag (e and f) and Chydrogel-Ag (g and h) nanocomposites with different magnifications.

The mechanism of the bactericidal effect of Ag based nanocomposite can be defined that Ag nanoparticles attach to the cell membrane

and interact with phosphorous and sulfur having compounds and then inactive the bacteria [30]. Size, shape and medium of Ag

NPs have significant effect on their antibacterial activity[40]. Smaller Ag NPs with having of large surface display more bactericidal effect than the larger Ag NPs. Chydrogel can provide more stability to Ag NPs rather than hydrogel, resulting in a higher antibacterial activity. Additionally, Chydrogel have sulfide groups which can be have high ability for penetrate to cell wall and its antibacterial activity against *S. aureus* higher than that of *E. coli*. The second test was performed in Luria-Bertani (LB) medium on the solid agar petri dish. This method cannot study alone bactericidal and bacteriostatic effects, so the MIC of samples should measure. Fig. 5 shows the images of this method and confirms the result of the MIC. The growth in the

inhibition ring of *E. coli* treated by Chydrogel-Ag nanocomposite (Fig 5d) and hydrogel-Ag nanocomposite (Fig 5e) were 16 and 12 mm while inhibition rings of *S. aureus* treated by these compounds were 18 and 13 mm (Fig 5d and e), respectively. As shown in Fig. 5, pure hydrogel and Thydrogel display no inhibition bacterial growth (Fig 5 a and b) and these confirms the results of MIC method. For comparison, antibacterial activity of Ag NPs on Thydrogel before adjusting of pH of hydrogel against *E. coli* was shown (Fig 5c). The inhibition ring of *E. coli* was 13 mm that this increase of antibacterial activity could be related to the size of Ag NPs.

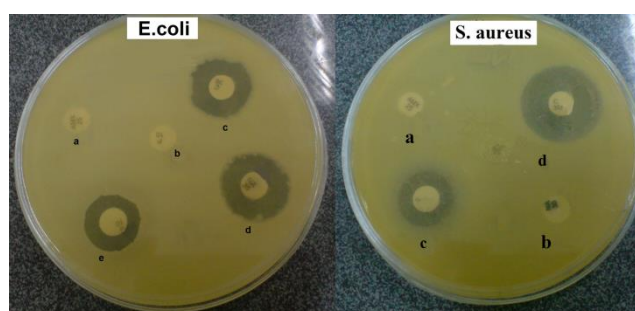


Fig. 5. A: Antibacterial activity of hydrogel (a), hydrogel-Ag (b), Chydrogel (c) Chydrogel-Ag before adjust pH (d) final Chydrogel-Ag (e) against *E. coli* and *S. aureus*, respectively.

Conclusions

In summary, Ag NPs were prepared in PAA and Cys modified PAA hydrogel networks and then was studied the effect of Cys molecules on the morphology and

antibacterial behavior of nanocomposites. Nanocomposites were characterized by several methods to confirm the formation of Ag NPs in hydrogel matrix and antibacterial study on *S. aureus* and *E. coli*. FT-IR and XRD analysis confirmed the

modification of hydrogel with cysteine and the loading of Ag NPs in hydrogel networks, respectively. The characterization of resulted nanocomposites was also performed through monitoring swelling behavior, FTIR spectroscopy, UV–Vis spectrophotometer and SEM. Meanwhile, antibacterial results showed that modified nanocomposite has well antibacterial activity against *S. aureus* than the other samples. Also, the results showed compared to hydrogel network, hydrogel has high swelling behavior but its nanocomposite has low swelling behavior.

References:

1. Adhikari B, Banerjee A (2010) *Chem. Eur. J.* **16**:13698-13705.
2. Zhu J, Aruna S, Koltypin Y, Gedanken A (2000) *Chem. Mat.* **12**:143-147.
3. Shervani Z, Ikushima Y, Sato M, Kawanami H, Hakuta Y, Yokoyama T, Nagase T, Kuneida H, Aramaki K (2008) *Colloid. Polym. Sci.* **286**:403-410.
4. Chen C, Wang L, Yu H, Wang J, Zhou J, Tan Q, Deng L (2007) *Nanotechnology* **18**:115612.
5. Zhu J, Liu S, Palchik O, Koltypin Y, Gedanken A (2000) *Langmuir* **16**:6396-6399.
6. Abdelwahed W, Degobert G, Stainmesse S, Fessi H (2006) *Adv. Drug. Deliv. Rev* **58**:1688-1713.
7. Wahab MA, Islam N, Hoque ME, Young DJ (2018) *Curr. Anal. Chem.* **14**: 198-202
8. Philip D (2009) *Spectrochim. Acta. A Mol. Biomol. Spectrosc.* **73**: 374-381.
9. Perdikaki A, Galeou A, Pilatos G, Karatasios I, Kanellopoulos NK, Prombona A, Karanikolos GN (2016) *ACS. Appl. Mater. Interfaces.* **8**:27498-27510.
10. Li W-R, Xie X-B, Shi Q-S, Zeng H-Y, You-Sheng O-Y, Chen Y-B (2010) *Appl. Microbiol. Biotechnol.* **85**:1115-1122.
11. Bajpai S, Mohan YM, Bajpai M, Tankhiwale R, Thomas V (2007) *J. nanosci. nanotechno.* **7**:2994-3010
12. Thomas V, Namdeo M, Murali Mohan Y, Bajpai S, Bajpai M (2007) *J. Macromol. Sci. Pure. Appl. Chem.* **45**:107-119
13. Hebeish A, Hashem M, El-Hady MA, Sharaf S (2013) *Carbohydr. Polym.* **92**:407-413
14. Fathalipour S, Pourbeyram S, Sharafian A, Tanomand A, Azam P (2017) *Mater. Sci. Eng. C.* **75**:742-751
15. Fathalipour S, Abdi E (2016) *Synth Met.* **221**:159-168
16. Fathalipour S, Mardi M (2017) *Mater. Sci. Eng. C.* **79**:55-65
17. Mohan YM, Vimala K, Thomas V, Varaprasad K, Sreedhar B, Bajpai S, Raju

- KM (2010) *J. Colloid. Interface. Sci.* **342**:73-82
18. Kamoun EA, Kenawy E-RS, Chen X (2017) *J. Adv. Res.* **8**:217-233
19. Peppas NA, Khare AR (1993) **11**:1-35
20. Sun Z, Lv F, Cao L, Liu L, Zhang Y, Lu Z (2015) *Angew. Chem. Int. Ed* **54**:7944-7948
21. Basit H, Pal A, Sen S, Bhattacharya S (2008) *Chem. Eur. J.* **14**:6534-6545
22. Murthy PK, Mohan YM, Varaprasad K, Sreedhar B, Raju KM (2008) *Colloid. Interface. Sci.* **318**:217-224
23. Mohan YM, Lee K, Premkumar T, Geckeler KE (2007) *Polymer* **48**:158-164
24. Varaprasad K, Mohan YM, Ravindra S, Reddy NN, Vimala K, Monika K, Sreedhar B, Raju KM (2010) *J. Appl. Polym. Sci.* **115**:1199-1207
25. Fullenkamp DE, Rivera JG, Gong Y-k, Lau KA, He L, Varshney R, Messersmith PB (2012) *Biomaterials* **33**:3783-3791
26. Sahraei R, Ghaemy M (2017) *Carbohydrate polymers* **157**:823-833
27. Mulvaney P (1996) *Langmuir* **12**:788-800
28. Vetter A, Reinisch A, Strunk D, Kremser C, Hahn H, Huck C, Ostermann T, Leithner K, Bernkop-Schnürch A (2011) *J. drug. target.* **19**:562-572
29. Babu VR, Kim C, Kim S, Ahn C, Lee Y-I (2010) *Carbohydrate Polymers* **81**:196-202
30. Chandra Babu A, Prabhakar M, Suresh Babu A, Mallikarjuna B, Subha M, Chowdoji Rao K (2013) *Int. J. Carbohydr. Chem.* **2013**:1-8.
31. Varaprasad K, Vimala K, Ravindra S, Reddy NN, Raju KM (2011) *Polym. Plast. Technol. Eng.* **50**:1199-1207
32. Pourjavadi A, Ghasemzadeh H, Mojahedi F (2009) *J. Appl. Polym. Sci.* **113**:3442-3449
33. Wu J, Lin J, Zhou M, Wei C (2000) *Macromol Rapid. Commun.* **21**:1032-1034.
34. Toda M, Stefan T, Simon S, Balasz I, Daraban L (2014) *Turk. J. Phys.* **38**:261-267
35. Mao H, Bell P, Shaner Jt, Steinberg D (1978) *J. Appl. Phys.* **49**:3276-3283
36. Massoumi B, Fathalipour S (2014) *Polym.Sci. Ser A* **56**:373-382
37. Sahu D, Acharya B, Panda A (2011) *Ultrason. sonochem.* **18**:601-607
38. Arndt K, Richter A, Ludwig S, Zimmermann J, Kressler J, Kuckling D, Adler H (1999) *Acta. Polym.* **50**:383-390
39. Choudhury A (2009) *Actuator B.Chem.* **138**:318-325
40. Sharma VK, Yngard RA, Lin Y (2009) *Adv. Colloid. Interface. Sci.* **145**:83-96.